

## Paramagnetic Meissner effect in Nb

P. Kostić, B. Veal, A. P. Paulikas, U. Welp, V. R. Todt, C. Gu, U. Geiser, J. M. Williams, K. D. Carlson, and R. A. Klemm  
*Materials Science Division, Argonne National Laboratory, Argonne, Illinois 60439*

(Received 7 August 1995; revised manuscript received 15 September 1995)

The paramagnetic Meissner effect (PME), or Wohlleben effect, in which the field-cooled magnetization of superconducting samples is paramagnetic below  $T_c$ , has been reported to occur in some samples of a variety of high- $T_c$  cuprate superconductors. It has been proposed that the effect arose in granular hole-doped cuprates from current loops with  $\pi$  phase shifts of the superconducting order parameter at some grain-boundary junctions. It is argued that such behavior would be expected to occur in a  $d$ -wave superconductor, but not in a conventional  $s$ -wave superconductor. To test this hypothesis, we have searched for the occurrence of the effect in Nb, and have confirmed a recent report by Minhaj *et al.* of its occurrence in some Nb samples. For these studies, the effects of stray fields and field gradients in the measurement volume of the superconducting quantum interference device magnetometer have been carefully considered to rule out the possibility that measurement artifacts might be responsible for the apparent paramagnetic behavior in Nb. The  $M(T)$  and  $M(H)$  curves obtained in Nb samples that show the PME also show remarkably strong resemblance to those curves reported for the cuprate materials exhibiting the PME. Evidence is presented that the effect arises from inhomogeneously trapped flux, and is strongly influenced by sample geometry and surface effects. These results suggest that, for the effect to be observable,  $T_c$  on the sample surface must be different from the bulk  $T_c$ . The occurrence of the PME in Nb strongly suggests that the observation of this effect is unrelated to  $d$ -wave superconductivity.

### I. INTRODUCTION

In addition to zero resistance below the transition temperature  $T_c$ , the second defining property of ordinary superconductors is the Meissner effect. When a superconducting sample is cooled in a magnetic field  $\mathbf{H}$  to a temperature  $T$  below  $T_c$  (or  $T_{c1}$  in the case of type-II superconductors) ideally all magnetic flux is expelled, and the sample behaves like a perfect diamagnet, i.e., its susceptibility  $\chi$  is  $-1/4\pi$ . Because some flux pinning is always present in real samples, flux expulsion is incomplete; the sample goes diamagnetic, but with a susceptibility magnitude  $|\chi|$  less than  $1/4\pi$  and can exhibit some amount of hysteresis.<sup>1</sup> Recently, however, a number of workers have reported observations of an unusual low-field magnetic behavior in some samples of cuprate superconductors.<sup>2-8</sup> In these samples, the zero-field-cooled (ZFC)  $\chi$  was diamagnetic, as in conventional materials, but the field-cooled (FC)  $\chi$  was found to be *paramagnetic*, or positive, below  $T_c$ . This effect has since come to be known as the paramagnetic Meissner effect (PME) or Wohlleben effect.

One of the earlier experiments<sup>3</sup> reported measurements using a commercial (Quantum Design, Inc.) superconducting quantum interference device (SQUID), in which the sample is moving during the measurement. It has been argued that, for such a system, the reported paramagnetism could have been due to an artifact of the measurement.<sup>9</sup> However, several authors<sup>4-7</sup> have since used SQUID magnetometers in which the sample is not moved during the measurement, so as to avoid that particular pitfall, and still claim to see the effect.

Observation of the PME has been reported in films and single crystals as well as sintered and melt-textured polycrystalline samples of cuprate superconductors. Typically, the

effect is observed in only a relatively small number of measured samples. Samples of  $\text{Bi}_2\text{Sr}_2\text{CaCu}_2\text{O}_{8+\delta}$  (Bi2212) which showed the effect were either sintered<sup>2</sup> or melt-processed polycrystalline,<sup>4</sup> with the latter exhibiting the largest paramagnetic signals. In the Bi2212 samples, the grains were very flat, and the  $c$  axes for a significant fraction of the grains were mutually aligned. In the measurements,  $\mathbf{H}$  was applied normal to the flat grain surfaces. There are two reports of PME in single-crystal samples for  $\mathbf{H}\parallel c$ , namely in  $\text{La}_2\text{CuO}_{4+\delta}$  (Ref. 7) and in  $\text{YBa}_2\text{Cu}_3\text{O}_{7-\delta}$  (YBCO).<sup>6</sup> A substantial effect was observed<sup>8</sup> with  $\mathbf{H}\parallel c$  in  $c$ -axis-oriented  $\text{HoBa}_2\text{Cu}_3\text{O}_{7-\delta}$  films and in polycrystalline, pressed pellet  $(\text{Er}_{0.2}\text{Ca}_{0.8})\text{Sr}_2(\text{Tl}_{0.5}\text{Pb}_{0.5})\text{Cu}_2\text{O}_y$  samples.<sup>3</sup> The magnitude of the PME varies from more than 50% of  $1/4\pi$  (50% of the magnitude of full flux expulsion) in melt-processed Bi2212 to less than 3% in YBCO single crystals.

One proposed explanation<sup>10-14</sup> for the origin of the PME is based on the idea that Josephson coupling between grain boundaries can result in spontaneous current loops originating from  $\pi$  junctions at some of the grain boundaries. Sigrist and Rice<sup>10</sup> considered a single wire loop containing either a single 0 junction or a single  $\pi$  junction. For the 0 junction, the current for Josephson tunneling across the junction could be written as  $I=I_c \sin\delta$ , where  $\delta$  is the phase difference of the superconducting order parameter on the two sides of the junction, which depends upon the magnetic flux trapped in the ring. In this 0-junction case, the free energy was minimized if no current spontaneously flowed in the ring, and hence no magnetic flux was spontaneously trapped in the loop. For a  $\pi$  junction, however,  $I=-I_c \sin\delta$ , which could be written as  $I=I_c \sin(\delta+\pi)$ , corresponding to an additional relative phase shift of  $\pi$  across the junction. Sigrist and Rice<sup>10</sup> showed that the free energy was minimized if a spontaneous current flowed in the ring, creating a magnetic flux

equal to one-half of a flux quantum  $\Phi_0$  in the area enclosed by the ring. They then argued that if the granular cuprate sample exhibiting the PME consisted of a substantial collection of Josephson junctions at the points of nearest contact of the grain, and if a substantial fraction of these junctions were  $\pi$  junctions, then a significant amount of spontaneous current and corresponding amount of flux *opposite* in sign to the applied field direction could be produced, and could account for the large PME magnitudes observed in granular Bi2212 samples. Simulations by Domínguez, Jagla, and Balseiro<sup>11</sup> were supportive of this contention, resulting in magnetization  $M(T)$  curves that exhibited the dip just below  $T_c$ , followed by the gradual saturation to large paramagnetic values in the “ $T_p$ ” regime, as observed.<sup>2–5</sup> For this explanation to be valid, the orbital pair wave function must be very anisotropic, changing sign about a center of symmetry. In Refs. 10–14, the order-parameter symmetry was considered to be  $d$  wave.

To test the validity of this explanation we looked for the PME in disks of elemental Nb cut from a variety of source materials. Nb is generally considered to be a conventional superconductor, exhibiting the usual BCS  $s$ -wave order parameter and isotropic gap function. If the paramagnetic effect could be observed in Nb, then the PME can have a conventional explanation and may not require a  $d$ -wave or exotic pairing mechanism. We consistently observe the PME in Nb disks cut from some sheets of rolled Nb. Disks cut from other source materials do not show the effect. The  $M(T)$  and  $M(H)$  of the PME Nb samples are remarkably similar to those reported for the PME cuprate superconductors. The PME in our Nb samples is very sensitive to the details of the sample surface and geometry. In particular, we present evidence that the surface layers of the PME samples have a different  $T_c$  than the bulk, and that removal of these surface layers removes the PME as well. These results confirm a recent report by Minhaj *et al.*<sup>15</sup> who observed the effect in inhomogeneous samples of Nb that show very broad or multiple superconducting transitions. Thompson *et al.*<sup>15</sup> observed that  $T_c$ 's on the sample surfaces were lower than  $T_c$ 's of the bulk. We have observed similar behavior in samples cut from one source of rolled Nb. PME samples cut from another source of rolled sheet show  $T_c$ 's on the sample surfaces that are apparently higher than  $T_c$ 's of the underlying bulk. The latter behavior (PME associated with a high surface  $T_c$ ) was also reported by Lucht *et al.*<sup>18</sup> on measurements of single-crystal YBCO. It appears that the PME can be found (perhaps quite generally) in samples showing strong flux pinning if the sample surface is appropriately altered relative to the bulk. We speculate that the effect might be a result of flux compression, possibly aided by strong surface pinning, that might develop as the sample cools through  $T_c$ .

We have extensively checked our experiment for artifacts (stray fields, nondipolar response, etc.). Details of these studies are given in the Appendixes.

## II. EXPERIMENTAL

### A. Samples

A variety of Nb samples were prepared for this study. Some showed the PME effect, some did not. All of these were disk-shaped, with diameters from 3 to 6 mm, and vary-

ing in thickness from 25  $\mu\text{m}$  (1 mil foil) to 1.8 mm. Samples that did not show the effect include: (1) A 3 mm diameter sample (labeled JW) prepared from ultrahigh-purity Nb, by rolling a Nb ball (of nominally 99.9999% purity) between sheets of 99.99% Nb, to a thickness of  $\sim 0.2$  mm, (2) disk samples, from Materials Research Corp., 0.3–1.6 mm thick, sliced from 1/4 in. diameter rod (labeled BV), with specified purity 99.8%, and (3) disks, 6 mm in diameter, cut from one mil thick Nb foil of unknown purity.

Samples that reliably showed the PME came from two different batches of commercial cold rolled Nb sheet of unknown origin, purchased between 5 and 30 years ago, with thicknesses 0.25 and 0.51 mm (10 and 20 mils). A chemical analysis of the 0.25 mm sheet (labeled KG) showed this material to be no more than 99.9% pure. (The Nb could be significantly less than 99.9% pure owing to contaminants not determined, i.e., elements lighter than the first row transition elements.) Ta and W were the principal contaminants in concentrations totaling  $\sim 800$  ppm. The  $T_c$  values for all Nb samples in this study were 9.2 K or higher, with transition widths of 0.2 K or less. The 0.51 mm sample was labeled BK.

### B. SQUID magnetometers

Essentially all results that we report here were obtained from a noncommercial low-field instrument<sup>16</sup> which we designate SQUID No. 1. However, one sample (KG) which showed a strong PME, was also measured in a commercial instrument manufactured by Quantum Design, Inc. We designate this instrument SQUID No. 2.

Generally, samples were placed in the SQUID's with the applied  $\mathbf{H}$  oriented parallel to the disk axis. Because of demagnetization factors, this orientation gives the largest signal for a given applied  $H$ . The magnitude of  $M$  was calibrated previously by measuring it for a Pb sphere in the Meissner state and for a soft ferromagnetic sphere.

In the low-field SQUID No. 1, the detection system consists of two balanced counterwound superconducting coils, axially oriented, with the sample normally located at the center of the upper coil. The positions of the coils are at approximately  $z=50$  and 60 mm relative to a fiducial mark on the sample probe. When a superconducting sample is cooled in an applied  $H$  through its  $T_c$ , magnetic flux is normally expelled from the sample and a current is induced in the pickup coil which is fed to the SQUID and detected. In the usual mode of operation, diamagnetism or paramagnetism is determined by the sign of the induced signal, monitored as  $T$  is swept through  $T_c$ . Since it is much easier to control the warming rate than the cooling rate in this system, measurements were normally taken with the sample warming after cooling in the appropriate  $\mathbf{H}$ . In order to avoid stray magnetic fields caused by the heater current, the sample heater was not used for these measurements. The sample was allowed to warm slowly as a result of heat leaks into the system. With this procedure, the sample is not moved during the course of the measurement. The magnetic response was readily studied vs  $T$  with  $H$  between 0.01 and 50 Oe.

Measurements with a stationary sample avoid problems which can be caused by moving the sample through a potentially nonuniform applied  $\mathbf{H}$ . However, measurement fields in the PME experiments are sometimes very small (e.g.,

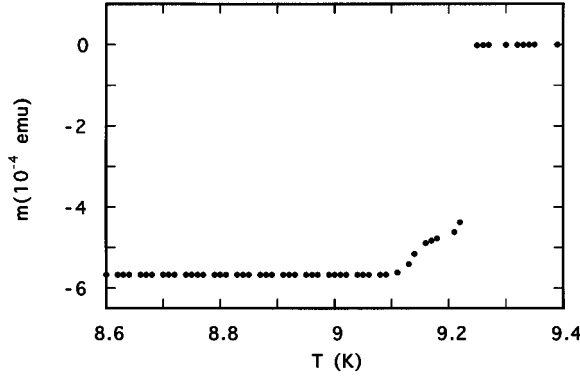


FIG. 1. ZFC magnetization versus  $T$ , measured in  $H=0.1$  Oe, for a Nb sample (KG-y) cut from a sheet 0.25 mm thick. This sample shows a strong paramagnetic Meissner effect. The superconducting transition occurs within 0.2 K temperature interval but shows two apparent  $T_c$ 's.

mOe). Thus, care must be taken to insure that effects of residual fields  $\mathbf{H}_r$  are eliminated (see Appendix A). Further, stationary sample results do not allow one to judge whether the observed signal is really a reflection of a magnetic dipole moment or if it is caused by some distorted  $M$  distribution. By scanning the sample through the superconducting pickup coils and analyzing the resulting traces we confirmed that the Nb discs can show paramagnetic dipole moments in the Meissner state. The results were corroborated in SQUID No. 2.

In SQUID No. 2, the sample moves vertically between detection coils during the measurement. A central coil is axially located between two counterwound coils, with each outer coil containing half the turns of the central coil. The magnetic moment is determined, at a fixed  $T$ , by fitting a function with the character expected from a dipole sample to the observed signal which is oscillatory in the vertical position.  $M(T)$  is obtained from a series of such measurements.

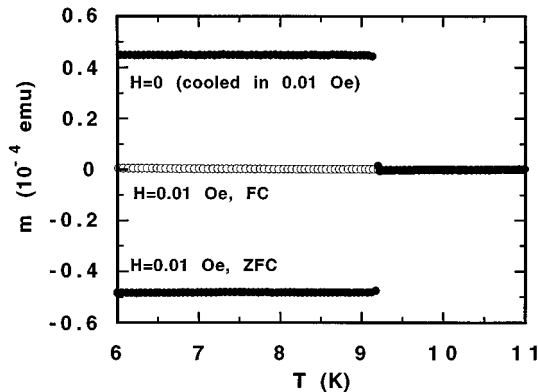


FIG. 2. Magnetization versus  $T$ , measured on warming, of a disk-shaped Nb sample (BV), 6 mm in diameter and 0.25 mm thick, cut from an ingot. Lower curve: ZFC, measured in  $H=0.01$  Oe. Upper curve: FC in 0.01 Oe, measured in zero field (trapped flux). Open circles: FC and measured in  $H=0.01$  Oe. These results show that flux pinning is very strong. As the sample cools through  $T_c$ , little flux is expelled and the field-cooled magnetization signal is extremely weak.

The low-field SQUID No. 1 contains double mumetal shielding to minimize effects from the earth's and other stray fields. SQUID No. 2 is not magnetically shielded. Thus, the earth's magnetic field ( $\sim 0.5$  Oe) and other external fields of unknown origin, might appear within the measurement volume. From SQUID No. 2, we consider only those measurements taken at fields of 5 Oe or higher, where effects of stray fields are sufficiently small.

To investigate the effects of residual stray fields and field gradients, the system response of SQUID No. 1 was extensively studied at fixed  $T < T_c$  as the sample vertical position  $z$  along the axis of the two detection coils was varied (see Appendix A). A procedure was devised to measure the residual field  $H_r(z)$  and axial field gradient  $H'_r(z) = dH_r(z)/dz$  within the measurement volume. We found that  $H_r(z)$  varied by about 4 mOe between detection coils. This stray  $H_r$  was found to distort the dipole signal, sometimes confusing the apparent sign of the response. By subtracting  $H_r$ , such ambiguities were removed.

### III. RESULTS

#### A. Shielding and remnant flux measurements

In Fig. 1, obtained from SQUID No. 1, we show a shielding measurement; i.e., the ZFC (zero-field-cooled)  $M(T)$  for a sample (KG-y) that shows a strong PME. The sample was cooled in  $H=0$ , and measured on warming in  $H=0.1$  Oe. This sample exhibits the full diamagnetic signal expected for the ZFC measurement. Note that the transition is sharp, occurring within  $\sim 0.15$  K. However, a clearly defined step is visible indicating the presence of two distinct transitions.

In Fig. 2, the low-field  $M(T)$  for a Nb sample (BV) is shown. These data were obtained from a disk-shaped Nb sample, 6 mm diameter and 0.25 mm thick, cut from an ingot. The lower curve shows the (diamagnetic) ZFC curve, measured in 0.01 Oe; i.e., the (essentially complete) exclusion of the flux imposed on the sample after cooling it below  $T_c$ . The upper curve represents  $M(T)$  measured on warming, with  $H=0$ , after cooling below  $T_c$  in 0.01 Oe. This curve measures the flux retained by the FC sample, when  $H$  is subsequently removed below  $T_c$ . This signal is comparable in magnitude to the ZFC trace indicating that nearly all flux penetrating the sample above  $T_c$  has been trapped at  $T < T_c$ . The open circles are the FC  $M$ , when the sample is both cooled and measured (warming) in 0.01 Oe. The FC data are roughly equivalent to the sum of the ZFC data and the  $H=0$  data taken after cooling in 0.01 Oe. Thus, while this sample does not show a PME, it displays very strong flux pinning and a very small FC signal, behavior typical of all the Nb samples that we studied. For different Nb samples with different surface preparations, we find that the small FC signal is sometimes positive (paramagnetic), and other times weakly diamagnetic.

Note, also, that the transition in Fig. 2 is very sharp (less than 0.05 K) and *does not show the foot associated with a second transition*, as found in Fig. 1. We have repeatedly observed that the paramagnetic behavior is associated with a double transition; if the transition is sharp and singular, we do not observe the PME.

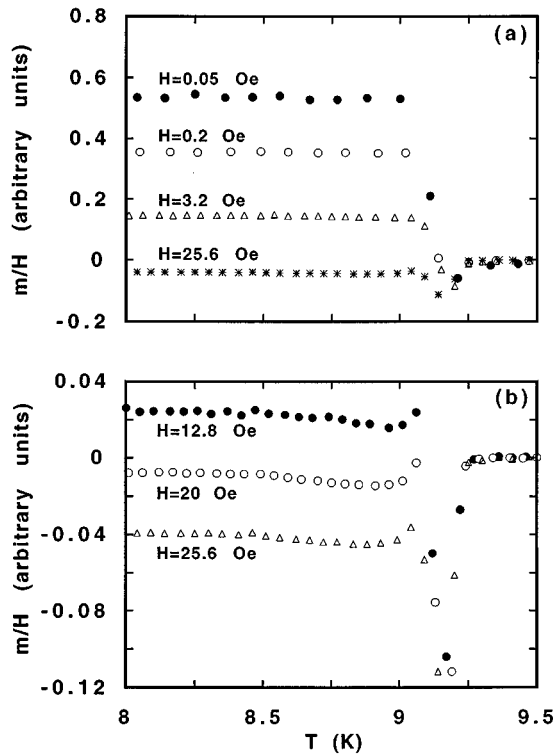


FIG. 3. Field-cooled susceptibility ( $M/H$ ), measured on warming, versus  $T$  for a disk-shaped Nb sample (KG-1), 6 mm in diameter and 0.25 mm thick, cut from a rolled sheet. Fields in which measurements were taken are indicated on the curves. For  $H=25.6$  Oe, the response is diamagnetic, but becomes paramagnetic at fields below 20 Oe.

### B. Field-cooled magnetization—surface and bulk superconductivity

A series of FC  $M$  measurements, obtained in SQUID No. 1, for a 6 mm diameter Nb disk (sample KG-1) with disk axis parallel to the applied field, are shown in Fig. 3. After positioning the sample in the upper pickup coil at  $z=60$  mm, the sample was cooled, in the specified field, and measured while warming through  $T_c$ . The sample was not moved until the measurements were completed. The FC susceptibility  $\chi(T) = M(T)/H$  is shown in the vicinity of  $T_c$ . In Fig. 3(a)  $\chi$  is shown for four  $H$  values, over the range 8 K  $< T < 9.5$  K. For  $H=25.6$  Oe, the response is diamagnetic, but as  $H$  is successively reduced to the values 3.2, 0.2, and 0.05 Oe,  $\chi$  is increasingly *paramagnetic*. Note further that all of these data exhibit a dip just below  $T_c$ , followed by a rise in  $\chi$  to some particular saturation value. For the three cases in which this saturation value is paramagnetic, we denote the  $T$  at which this occurs as  $T_p$ , as it is quite well-defined, precisely as in the single crystal of YBCO which exhibited the PME.<sup>6</sup> Shown in Fig. 3(b) is a detail of the transition region, with  $\chi$  curves at  $H=25.6$ , 20, and 12.8 Oe. A diamagnetic onset occurs for all three fields at precisely the same value, 9.25 K, very close to the bulk  $T_c$  of high-purity Nb.<sup>17</sup> A  $\chi$  minimum occurs at roughly 9.15–9.20 K in all three data sets, and at lower  $T$  values,  $\chi$  increases to a maximum at about 9.06 K. For the two larger  $H$  values in Fig. 3(b), this maximum is not paramagnetic, and  $\chi$  remains diamagnetic for all  $T < T_c$ . Below  $\sim 8.5$  K,  $\chi$  becomes independent of  $T$ . The behavior

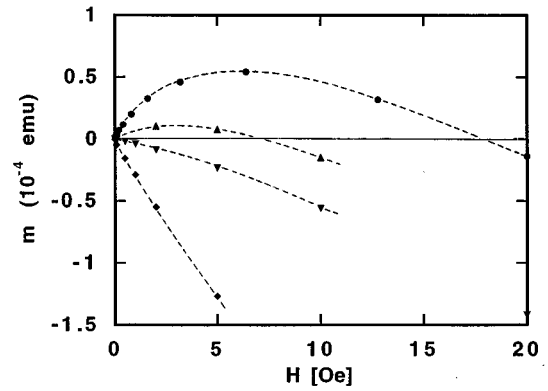


FIG. 4.  $M(H)$  curves for a series of Nb samples. Curves, from top to bottom, were obtained from samples KG-1, BK, JW, BV. The KG and BK samples were cut from rolled sheet stock, the JW and BV samples were cut from ingots.

shown in Fig. 3 is remarkably similar to that obtained in a single crystal of YBCO, as pictured in Fig. 1(b) of Ref. 6.

In Fig. 4,  $M(H)$  at low  $T$  ( $\sim 7$  K) from the same sample as shown in Fig. 3 is plotted (top curve). At low  $H$ ,  $M(H)$  increases almost linearly. The slope decreases with increasing  $H$ , with a maximum in  $M(H)$  appearing at about 6–7 Oe;  $M(H)$  becomes negative at about 18 Oe. This behavior is very similar to that pictured in Fig. 6 of Ref. 6 (sample 1) with  $H \parallel c$  in single-crystal YBCO. Also shown in Fig. 4 are  $M(H)$  measurements for three other Nb samples (BK, JW, and BV) described in Sec. II A. These show much weaker, or no paramagnetism.

Figure 5(a) (solid circles), shows the FC  $M$  measured in 1 Oe on a disk-shaped commercial rolled sample 6 mm in diameter, 0.5 mm thick (sample BK), prepared by cutting from a sheet with scissors. This paramagnetic sample exhibits the usual dip below  $T_c$ , followed by the rapid rise to a rather constant value below  $T_p$ . Following that measurement (solid circles), the sample was removed, and the faces were polished using 0.1  $\mu\text{m}$  diamond polishing grit. The sample was remeasured. The data are pictured as the solid triangles in Fig. 5(a). Curiously, polishing the surfaces has caused the PME to *disappear entirely*. Although we were not aware of this behavior having been observed by others at the time of measurement, the recent work of Thompson *et al.*<sup>15</sup> on Nb has reached the same empirical conclusion: that the PME is strongly sensitive to the surface microstructure, and can disappear with polishing. In another sample we cut from a sheet, the PME disappeared upon polishing the edge (circumference) of the sample.

The data in Fig. 5(a) suggest that the surface  $T_c$  is higher for the unpolished sample than for the sample with faces polished. To check this point, ZFC measurements (recorded in 0.01 Oe) were taken for the unpolished (solid circles) and polished (solid triangles) samples. Results are shown in Fig. 5(b). Additional ZFC results taken in 0.05 Oe for another sample cut from the same (BK) material are pictured in the inset of Fig. 5(b). Consistent with Fig. 5(a), a shift in  $T_c$  ( $\sim 0.1$  K) is observed between these measurements. [The onset of diamagnetism appears to occur at a slightly lower  $T_c$  for the FC measurements (upper panel), which were made at

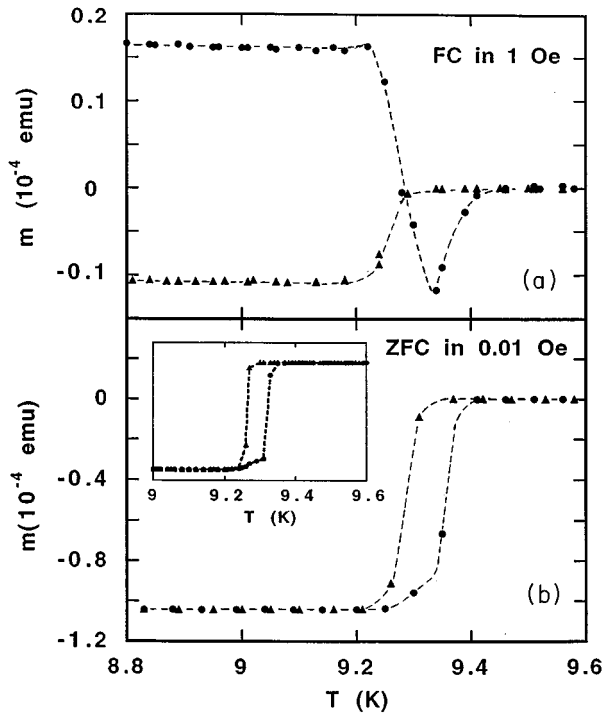


FIG. 5. (a) Solid circles: FC magnetization measured in 1 Oe from sample BK. Solid triangles: FC magnetization measured in 1 Oe after both faces of the sample were polished. (b)  $T_c$  measurements from ZFC measurements in 0.01 Oe. The solid circles (triangles) were taken before (after) polishing the sample faces. Inset: a high point density ZFC measurement at 0.05 Oe from another sample cut from the BK material.

1 Oe, compared to the 0.01 Oe measuring field for the ZFC measurements (lower panel).] The apparent shift of  $T_c$  between the polished and unpolished samples could occur if the  $T_c$  of the surface layer of the unpolished sample were higher than that of the bulk. Lucht *et al.*<sup>18</sup> have observed similar behavior from single crystals of YBCO; that is, samples showing the PME had a surface superconducting layer with a  $T_c$  higher than that of the bulk. Thus, for both YBCO crystals and the (BK) Nb sheet samples, removing the high- $T_c$  surface layer caused the PME to disappear.

However, disk samples cut from sheet stock labeled KG showed somewhat different behavior. This material also showed a strong PME (even larger than the BK material). Like the BK stock, the ZFC measurement showed a distinct foot in the superconducting transition (Fig. 1). Figure 6(a) shows 4 Oe FC measurements from a Nb sample (KG material) before (circles) and after (triangles) polishing. Like sample BK [Fig. 5(a)], the PME has disappeared with polishing. Figure 6(b) shows ZFC measurements before (circles) and after (triangles) polishing. Unlike sample BK (Fig. 5), the onset of superconductivity (ZFC) is unchanged but the *foot* has now disappeared with polishing. These results suggest that the sample is stratified with a component on the sample surface that has a  $T_c$  lower than that of the bulk. This behavior is similar to that reported by Thompson *et al.*<sup>15</sup> We were able to find the PME only in samples that showed evidence of stratification. It appears, however, that the PME can occur in samples where the surface layer  $T_c$  is either higher or lower than the bulk  $T_c$ .

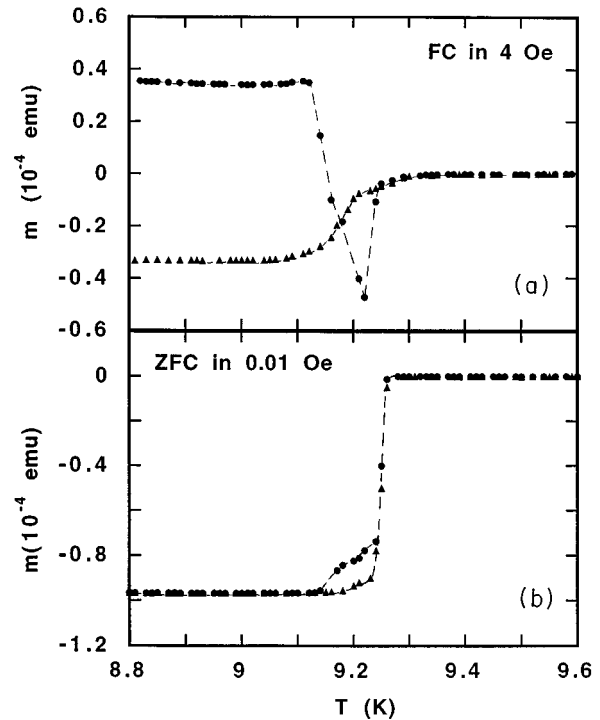


FIG. 6. FC (4 Oe) and ZFC (0.01 Oe) measurements on a Nb sample (KG material) taken before and after polishing the sample faces. Curve identification is the same as that in Fig. 5. Like sample BK (Fig. 5), polishing the sample faces eliminates the PME. However, unlike sample BK, polishing removes the low  $T_c$  foot (b) which is apparently associated with a surface layer.

Another feature that is repeatedly observed in FC samples which show the PME, is the strong diamagnetic overshoot which is visible just prior to the onset of paramagnetism (see Figs. 3, 5, and 6). As seen in Fig. 3(b), the overshoot can be very strong in these samples, even when the response is diamagnetic at the higher fields. Observe, however, that this overshoot behavior is strongly diminished or absent in the polished samples of Figs. 5 and 6, which do not exhibit the PME. This correlation (strong overshoot in samples exhibiting the PME, no overshoot if the PME is absent) appears to be quite robust. The indication from these measurements is that the altered surfaces in the rolled Nb sheet might be responsible both for the PME and for this overshoot behavior.

Apparently, the Nb samples most likely to show the PME have relatively low ( $\sim 99.9\%$ ) Nb purity and may have substantial defect concentrations resulting, for example, from cold working the material. Probably, strong flux pinning is a requirement for observation of the paramagnetic signal. We have observed that the magnitude of the paramagnetism can be substantially altered by smoothing the sample faces and edges, varying the sample purity or homogeneity, and changing the sample shape. While we have not observed FC paramagnetism at  $H > 0.1$  Oe in a survey of other superconductors, including A-15's, Pb, BSCCO, and YBCO, it may be that paramagnetism could be observed in these materials if attention were given to sample shapes and surface condition. In particular, as both Lucht *et al.*<sup>18</sup> and Thompson *et al.*<sup>15</sup> have argued, it appears that those samples which show the PME have a surface layer whose  $T_c$  is slightly different from

the  $T_c$  of the bulk. Our measurements on Nb strongly support this conclusion. Note, however, that the work of Lucht *et al.*<sup>18</sup> indicate that the surface  $T_c$  is higher than the bulk  $T_c$ , while Thompson *et al.*<sup>15</sup> conclude that the surface  $T_c$  is lower. Our studies have found that both of these conditions can be realized in Nb samples that show the PME. Results from a given source of rolled sheet Nb are robust, but can vary considerably with different sheet stock.

For additional confirmation of the paramagnetic behavior in Nb, sample KG-1 was sent to the University of Köln, Germany for additional study. The presence of the PME was confirmed.<sup>19</sup>

Samples exhibiting the PME have  $M(H)$  and  $M(T)$  curves that are remarkably similar to those obtained from single-crystal YBCO.<sup>6</sup> The main differences between the results obtained in this work for Nb and results obtained from melt-cast polycrystalline Bi2212 are (1) the magnitude of the effect, which is about two to three orders of magnitude smaller in our Nb samples (when measured at comparable fields), with  $\chi$  values on the order of 0.1–1% of  $1/4\pi$ , compared to 20–50% of  $1/4\pi$  in some cuprates, and (2) the sharpness of the dips in the  $M(T)$  curves in the vicinity of  $T_c$ . In melt-cast polycrystalline Bi2212, the  $M(T)$  curves are much more gradual.

#### IV. DISCUSSION

Paramagnetic effects at  $T_c$  have been observed in various circumstances. In 1943, Steiner and Schoeneck<sup>20</sup> reported  $M$  measurements on a Sn single crystal of several mm in thickness, and found that for weak applied current values, the FC  $M$  exhibited the usual Meissner effect, becoming fully diamagnetic. Upon using stronger applied currents and reducing  $T$  through  $T_c$ ,  $M(T)$  first became paramagnetic, and then went diamagnetic at a lower  $T$  value. They found that the effect was unaltered by reversing the current direction, although reversing the direction of  $\mathbf{H}$  changed the sign of the overall  $M$ , as expected. Similar results were later found by Meissner, Schmeissner, and Meissner in Sn and Hg samples.<sup>21</sup> While these authors were not able to determine the precise three-dimensional field and current density distributions in their samples, their results did at least indicate that current distributions different from those induced by diamagnetic shielding could give rise to a paramagnetic signal. We note that both Sn and Hg are type-I superconductors.

Later, experiments on wire samples of the type-II materials Nb and NbTa were performed by LeBlanc.<sup>22</sup> In these experiments, a current was passed along the wire, being sequentially added and removed. As this occurred, the static longitudinal magnetization alternated between paramagnetic and diamagnetic. LeBlanc proposed that the overall current formed helical paths in the wire, so as to maintain a constant inward Lorentz force density in the presence of the applied longitudinal magnetic field.

More recently, cylindrical samples of Pb doped with 1.0 at. % Tl were prepared by de la Cruz, Fink, and Luzuriaga.<sup>23</sup> These type-I samples had  $\kappa$  values of 0.54, which allowed for an  $H_{c3}$  exceeding the critical field  $H_c$  (since  $1.695 \kappa > 0.707$ ). The samples were then coated with chrome on part, none, or all of the radial surface, so as to prevent supercurrents from flowing in the surface sheath around the

sample. An  $\mathbf{H}$  parallel to the cylindrical axis was applied, and the sample cooled through  $T_c$ . In the uncoated samples, in the  $T$  regime between  $T(H_{c3})$  and  $T(H_c)$ , a supercurrent flowed in the surface of the sample, but the interior of the sample was normal. The resulting response was paramagnetic; they called the source of this paramagnetism a “giant vortex state.”<sup>23</sup> Below  $T(H_c)$ , the sample went fully diamagnetic. In the partially and fully coated samples, however, no such paramagnetic signal was observed. Thus, a paramagnetic signal could be obtained when surface currents could themselves trap the magnetic flux inside the core region of the sample. We note that in type-II materials, one will always have  $H_{c3} = 1.695H_{c2} > H_{c1}$ , so that  $T(H_{c3}) > T(H_{c1})$ , and the effect ought to be much more pronounced than in type-I materials, especially for large  $\kappa$  values, for which  $T(H_{c3}) \gg T(H_{c1})$ .

A possible explanation for the PME comes from inhomogeneous flux trapping that can occur during sample cooling. A diamagnetic signal is recorded in the magnetometer if flux is excluded, or moved outward, from the sample, as occurs in the usual Meissner effect. If, however, flux were compressed, for example, during the cooling process, in excess of the flux expulsion, then an apparent paramagnetic signal could be recorded.

Very recently, a flux compression mechanism has been investigated theoretically by Koshelev and Larkin (KL).<sup>24</sup> In their model, surface supercurrents inhomogeneously trap magnetic flux in the sample interior, as in the “giant vortex state”<sup>23</sup> (and perhaps in the earlier observations of paramagnetism<sup>20–22</sup>). They consider a sample in the shape of a long flat strip whose thickness  $d$  is much smaller than its width  $w$ . The length of strip is considered infinite, and  $\mathbf{H}$  is applied normal to the surface of the strip.<sup>25</sup> KL assume that in the FC state, the critical current density  $j_c$  flows in the central region of the strip of width  $2b$ , with  $|x| \leq b \leq w$ , and the surrounding regions of width  $w - b$  are flux free. Relative to the magnetization  $M_M = H/4\pi$  for full flux expulsion, KL found that  $M$  in the sample had the general form  $M/M_M = A + Bf$ , where  $f$  is the fraction of trapped flux compressed in the central region of the sample.  $A$  and  $B$  are functions of  $b/w$  involving elliptic integrals. In the limit  $b/w \rightarrow 0$ , they found that  $A \rightarrow -1$  and  $B \rightarrow 4/\pi$ . For full flux compression ( $f = 1$ ), the maximum  $M/M_M$  reduces to  $-1 + 4/\pi = 0.273$ , which is equivalent to a paramagnetic susceptibility of 27% of  $1/4\pi$ . In this situation of maximal flux compression,  $M$  is diamagnetic for  $f < \pi/4$ . KL also showed that most of the parameter space resulted in a diamagnetic response, but a paramagnetic response was always obtained for  $f = 1$ . In the limit  $b/w \rightarrow 1$ , however, the magnitude of the paramagnetic response vanished. Hence, for systems in which the flux free region is a small portion of the total sample volume (as might be expected for Nb samples much thicker than the penetration depth  $\lambda \sim 500 \text{ \AA}$ ), one expects a small PME. In very thin aligned Bi2212 micrograins (as are apparently present in the melt-cast polycrystalline samples<sup>4</sup>), this mechanism could lead to a PME of macroscopic proportions.

While it remains to be seen whether the KL model can be successfully applied to samples of different geometries (KL were able to obtain a solution for a disk-shaped geometry, but only in the limit  $w - b \ll w$ , for which the PME would be

small), KL have successfully shown that a single, simple mechanism, based solely upon the Maxwell equations, can explain the overall sign and magnitude of the PME, both in cuprate and in Nb samples.

Nevertheless, one aspect of the PME which is not well described by the KL model is the role of the sample surfaces. Since Thompson *et al.*,<sup>15</sup> Lucht *et al.*,<sup>18</sup> and this work indicate that polishing the samples causes the PME to disappear, it is not clear how this feature would be incorporated into the KL model. Since  $w-b$  could characterize the region of higher  $T_c$ , polishing the edge of the sample could reduce this region to zero, eliminating the effect. Otherwise, the only free parameter would be  $f$ , the fraction of flux trapped in the interior region. Perhaps by polishing the top and bottom surfaces, the flux in the interior region may become depinned, greatly reducing  $f$ , and driving the FC  $M$  diamagnetic. It remains to be seen if there might be some further experimental basis for either of these scenerios, however.

## V. SUMMARY

We have confirmed the existence of the paramagnetic Meissner effect in some samples of Nb. While the magnitude of the PME in Nb is considerably smaller than that observed in melt-cast Bi2212, the  $M(T)$  and  $M(H)$  curves obtained are remarkably similar to those obtained by Riedling *et al.*<sup>6</sup> on a single crystal of YBCO. A simple flux compression picture, resulting from inhomogeneous cooling through  $T_c$ , has been presented as a plausible explanation of the effect. Using this picture as a mechanism for achieving an inhomogeneous flux distribution, Koshelev and Larkin<sup>24</sup> have presented a simple model to explain how the PME can be large in some samples, small in others, and nonexistent in most samples (with  $f < \pi/4$ ). Polishing the sample surfaces, with consequent alteration of the PME, suggests that surface pinning of the magnetic flux plays an important role. There is also strong evidence that samples showing the effect have a surface  $T_c$  different from the bulk  $T_c$ . These observations lead us to conclude that the PME is likely to arise from inhomogeneously trapped flux, and is unlikely to have any relationship with  $d$ -wave superconductivity.

## ACKNOWLEDGMENTS

The authors would like to thank H. Claus, D. Khomskii, A. E. Koshelev, A. I. Larkin, D. J. Thompson, H. v. Löhneysen, and L. E. Wenger for useful discussions. This work was supported by the U.S. Department of Energy, Division of Basic Energy Sciences, under Contract No. W-31-109-ENG-38. One of us (C. Gu) was supported by the National Science Foundation, Science and Technology Center for Superconductivity, under Contract No. DMR 91-20000.

## APPENDIX A: RESIDUAL STRAY FIELDS AND GRADIENTS

These experiments involve measurements with small applied  $H$  values, and for the FC samples, a very small magnitude SQUID response. Consequently, it is a challenge to minimize measurement errors. Unless considerable care is taken with the measurements, even the observed sign (i.e., paramagnetism vs diamagnetism) can be incorrect. Problems

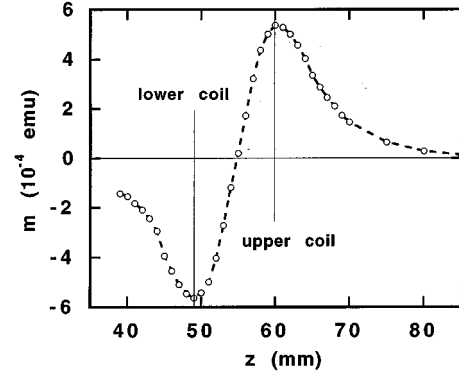


FIG. 7. The magnetization response  $S(z)$  of sample (KG-y) measured as a function of the position  $z$  along the vertical axis of the pickup coils in SQUID No. 1. The sample was measured in zero field, after cooling in 0.1 Oe (retained flux). This  $S(z)$  is the standard, nearly ideal dipole function showing peaks at  $z=49$  and  $60$  mm, the approximate locations of the pickup coils.

can arise from stray fields, from field inhomogeneities (e.g., resulting from inhomogeneities in the field coil), from inadequately balanced pickup coils and heater coils, and possibly from stray fields trapped in the superconducting pickup coils during the cooldown of the SQUID. In the presence of stray fields, inadvertent sample motion can introduce spurious signals. Errors from such sources encountered in a moving sample SQUID magnetometer have been previously considered.<sup>4,9</sup> Several papers have since emphasized that their data were taken using systems in which the samples were not moved during measurement; i.e.,  $M(T)$  was scanned through  $T_c$ . This may be a safer procedure for the detection of weak paramagnetic signals. Nonetheless for reliable low-field measurements, considerable care is required, even when the sample is not moved during the course of the measurement.

In the counterbalanced dual pickup coil system used here (SQUID No. 1), the signal from a superconducting sample (e.g., ZFC, measured in a small  $H$  at fixed  $T < T_c$ ) will change sign as the sample is repositioned vertically ( $z$  direction) from one coil to the other. The shielding response is  $S(z) = [f_1(z) - f_2(z)]\beta_2 H$  where  $\beta_2 = 1/4\pi$  for perfect diamagnetic shielding and the functions  $f_1(z)$  and  $f_2(z)$  give the shielding signal amplitudes in coils 1 and 2 as the sample is moved along  $z$ ;  $f_1(z)$  and  $f_2(z)$  are equivalent symmetrical functions but each is centered at its respective coil center. Figure 7 (open circles) shows  $S(z)$  from sample KG-y, which was cooled in 0.1 Oe (retained flux) at  $z=57.5$  mm, and then measured in  $H=0$  as a function of the sample vertical position  $z$ . The response  $S(z)$  is antisymmetric, both about zero magnetization and the center point between the coils, with minimum amplitude at  $z=49$  mm and maximum at 60 mm, the approximate positions of the lower and upper pickup coils, respectively. (The  $z$ -axis positions are measured relative to a fiducial mark on the sample probe.)

We have determined that a field gradient exists in the measurement volume of this system. The field varies by about 4 mOe between the pickup coils. We will see that this relatively small field gradient can seriously affect the measurements unless careful procedures are followed.

In Fig. 8(a), we show a series of measurements probing

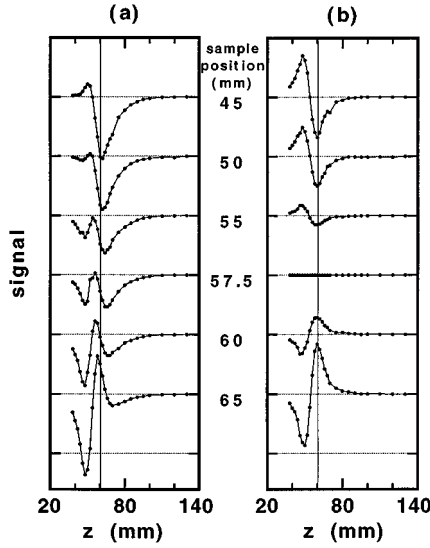


FIG. 8. (a) A series of measurements probing  $S(z)$  along the vertical axis of the pickup coils of SQUID No. 1 for a sample (BK) held at fixed temperature  $\sim 7$  K. For each of these curves, the sample was cooled, from  $T > T_c$ , in zero external field, with the sample at the vertical position indicated. (b)  $S(z)$  functions appearing in panel (a) after correcting for the field gradient. The corrected  $S(z)$  curves in panel (b) were obtained by simple subtraction of the  $S(z)$  function for  $z = 57.5$  mm from each curve of panel (a). All curves in this figure have the same scaling factor. The corrected curves in (b) are now the usual antisymmetric functions expected from a dipole sample. See text.

the magnetization response  $S(z)$  along the vertical axis  $z$  of the pickup coils for a Nb sample (BK) held at fixed  $T \sim 7$  K. For each of these curves, the sample was cooled, from  $T > T_c$ , in zero applied external field, with the sample at the vertical position indicated.  $S(z)$  was then measured with zero applied external field at different positions  $z$ . Since we obtain a position-dependent signal which varies with the location where the sample was cooled, it is clear that a spatially varying residual field  $H_r(z)$  exists between the pickup coils. If the sample were cooled in zero external field and  $H_r$  were zero everywhere between the coils, no signal  $S(z)$  would be observed. If a constant  $H_r$  existed between the coils, then after cooling in zero external field,  $S(z)$  would be independent of cooling position, the signal being a measure of the Meissner signal (flux expulsion) resulting from the constant  $H_r$ . However, for small constant  $H_r$ ,  $S(z) \approx 0$ , since the Nb samples show very little flux exclusion in a low-field FC measurement (Fig. 2), because the flux pinning is very strong. Consequently, the  $S(z)$  curves shown in Fig. 8(a), which are strongly dependent on the location where the sample was cooled, are sensing the residual field gradient  $H'_r(z) = dH_r(z)/dz$  in the measurement volume.

That is, to obtain the curves of Fig. 8(a), the sample was cooled in the  $H_r(z)$  at the specified  $z$  positions. The flux trapping is sufficiently strong so that the sample retains essentially the entire field in which it was cooled. Thus, as a (residual) FC sample of Fig. 8(a) is repositioned along  $z$ , a shielding response is generated that is proportional to the difference between the trapped field and the existing field at point  $z$ . Because of the varying  $H_r(z)$ , the response curves in

Fig. 8(a) do not show the desired antisymmetrical response expected from a dipole sample repositioned between the pickup coils (such as in Fig. 7).

We have seen that  $H'_r(z)$  provides substantial signal distortion. We now describe a procedure for measuring  $H'_r(z)$  and correcting for its effect on the response function  $S(z)$ . If we cool the sample in zero external field at position  $z_1$  (e.g., 50 mm), then measure the function  $S(z)$  at all points  $z$  [Fig. 8(a) is the function at 50 mm], we obtain for coil 1,  $S_{50}(z) = f_1(z)\beta_2[H_r(z) - H_{r1}]$  where  $H_{r1} = H_r(z_1)$ , and  $\beta_2 = 1/4\pi$ , assuming perfect shielding. The function  $f_1(z)$  gives the shielding signal amplitude in coil 1 as the sample is repositioned along  $z$ . Considering the signal from both (counterwound) coils, we have

$$\begin{aligned} S_{50}(z) &= f_1(z)\beta_2(H_r(z) - H_{r1}) - f_2(z)\beta_2(H_r(z) - H_{r1}) \\ &= [f_1(z) - f_2(z)]\beta_2(H_r(z) - H_{r1}). \end{aligned}$$

Now, we can define a ‘‘correction’’ function  $S_{\text{corr}}(z)$ , at all points  $z$ , obtained after cooling the sample in zero external field at position  $z_2$  (e.g., at 57.5 mm). In this case

$$\begin{aligned} S_{\text{corr}}(z) &= f_1(z)\beta_2(H_r(z) - H_{r2}) - f_2(z)\beta_2(H_r(z) - H_{r2}) \\ &= [f_1(z) - f_2(z)]\beta_2(H_r(z) - H_{r2}), \end{aligned}$$

where  $H_{r2} = H_r(z_2)$ . Thus the corrected response function obtained when the sample was cooled at 50 mm is

$$S(z) = S_{50}(z) - S_{\text{corr}}(z) = -[f_1(z) - f_2(z)]\beta_2(H_{r1} - H_{r2}). \quad (\text{A1})$$

The corrected function  $S(z)$ , obtained after cooling at  $z = 50$  mm, is a shielding (dipole) function for a sample sensing a constant field  $H_{\text{const}} = (H_{r1} - H_{r2})$  at all  $z$ .

Figure 8(b) shows the corrected  $S(z)$  functions obtained after the sample was cooled at the indicated  $z$  positions. That is, the measured  $S(z)$  curves in Fig. 8(a) were corrected by simple subtraction of the  $S(z)$  function [Fig. 8(a)] obtained after cooling the sample at  $z = 57.5$  mm. The corrected curves in Fig. 8(b) are now the usual antisymmetric functions expected from a dipole sample. We chose to use the  $S(z)$  function at  $z = 57.5$  mm for the correction function since, when the sample is cooled at this position and repositioned to the center of pickup coil 1 or coil 2, either pickup coil senses a comparable shielding signal from the change in field (i.e., the magnitude of the change in field from  $z = 57.5$  mm to the center of either coil is the same). Had the field gradient been exactly linear between the coils, this ‘‘central point’’ would have occurred midway between the coils, at  $z = 54.4$  mm instead of 57.5 mm. In Fig. 8(b), the antisymmetric  $S(z)$  signal inverts relative to the selected ‘‘zero point’’ obtained for a sample cooled at  $z = 57.5$  mm.

The maximum amplitude for each of the  $S(z)$  functions (i.e., the value at 60 mm) shown in Fig. 8(b) is proportional to the difference in the residual field at  $z$ , where the sample was cooled, from that at 57.5 mm [Eq. (1)]. Figure 9 (right scale) shows a plot of the maximum of  $S(z)$  for each curve of Fig. 8(b).

We now present procedures for measuring the absolute  $H_r(z)$  and  $H'_r(z)$ . In general, it is not straightforward to obtain accurate measurements of very small  $H_r$  (e.g., mOe lev-

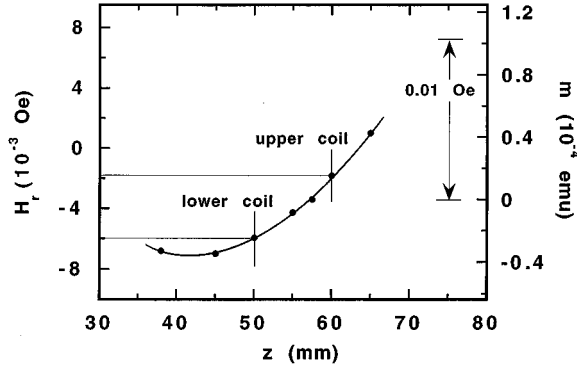


FIG. 9. Maximum of  $S(z)$  (right scale) for each curve of Fig. 8(b) and the associated vertical component of the residual magnetic field (left scale) within SQUID No. 1. The double arrow indicates the amplitude (right scale) associated with a known field of 0.01 Oe.

els) and  $H'_r(z)$  values in the measurement volume of the magnetometer. To accomplish this, we exploit the fact that flux trapping in the Nb samples is so strong that at low fields, such a sample retains essentially the entire field in which it was cooled. This property provides a sensitive capability for calibrating the  $H'_r(z)$  appearing between the pickup coils.

To calibrate  $H'_r(z)$  (Fig. 9) observed between the pickup coils, we position the sample at  $z=57.5$  mm, cool the sample in a known field, e.g., 0.01 Oe. Then, at  $T < T_c$ , set the external field to zero and record the axial response  $S(z)$ . Then, we subtract the  $S(z)$  obtained after cooling in zero external field at 57.5 mm [Fig. 8(a), response at 57.5 mm] to correct for  $H'_r(z)$ . This procedure yields the dipole response resulting from the flux retained in the sample after cooling in 0.01 Oe. The amplitude associated with a known 0.01 Oe field is shown by the double arrow in Fig. 9 (right scale).

We now describe a procedure to measure the absolute  $H_r$  at  $z=50$  and 60 mm, the approximate pickup coil positions. For these measurements, we exploit the Meissner effect, i.e., flux expulsion from a sample cooled in an external field. We use a single-crystal YBCO sample for which the FC diamagnetic signal  $\beta_1$  (expulsion) is about 6% of the ZFC (shielding) signal for  $H < 0.01$  Oe. In principle, it is sufficient to do two FC measurements at each coil position. For measurements 1 and 2 at one of the coil positions, we cool the sample below  $T_c$  in applied fields  $H_{a1}$  and  $H_{a2}$ , then measure  $S_1 = \beta_1[H_r + H_{a1}]$  and  $S_2 = \beta_1[H_r + H_{a2}]$ , the diamagnetic signals observed as the sample warms through  $T_c$ . Eliminating  $\beta_1$  yields  $H_r = [S_2 H_{a1} - S_1 H_{a2}] / [S_1 - S_2]$  at each coil. For optimal measurement sensitivity,  $H_r$  should be comparable in magnitude to  $H_{a1}$  and  $H_{a2}$ . For improved accuracy, the amplitude of the Meissner signal can be measured as a function of applied field  $H_a$  at each coil position, as shown in Fig. 10. Since the total field at the sample is  $H_r + H_a$ , zero Meissner signal implies  $H_r = -H_a$ . The measured  $H_r$  at  $z=50$  and 60 mm appear on the left-hand side of Fig. 9, and provide an absolute field calibration. Within 10%, these results are in agreement with the above  $H'_r(z)$  between the coils, measured by monitoring the shielding signals as the samples are repositioned in  $H_r(z)$ .

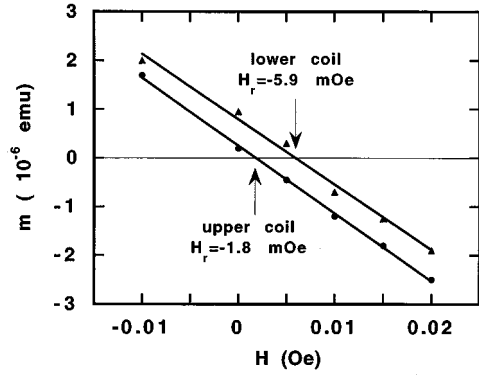


FIG. 10. Determination of the residual field at the coil positions of SQUID No. 1. The magnitude of flux expulsion (the Meissner signal) is measured as a function of applied field. At zero Meissner signal, the residual field is compensated by the applied field.

Note, in Fig. 10, that if measurements of  $M(T)$  were carried out at the lower coil position in  $H_a$  less than  $\sim 6$  mOe, a diamagnetic sample would erroneously appear to be paramagnetic, even when the sample was measured at fixed position. If, at a fixed  $|H_a|$ , pairs of  $M(T)$  measurements were taken with  $\text{sgn}(H_a)$  reversed, the difference of these  $M(T)$  functions should correct for  $H_r$ , yielding  $2M(T)$ , providing  $M(H, T) \propto H$ . However, a safer procedure is to carry out the measurements in a system with an accurately characterized  $H_r(z)$ .

## APPENDIX B: FIELD-COOLED MAGNETIZATION MEASUREMENTS

We now measure the FC  $M$  as a function of  $H_a$  for Nb disk sample KG-y. A simple procedure, discussed above, for measuring the FC  $M$  is to cool the sample in the desired  $H_a$ , while it is positioned in the plane of the upper detector coil, and then raise  $T$  through  $T_c$ . FC  $M(H)$  measurements obtained in this way appear in Fig. 4 (upper curve).

It is also instructive to examine the response functions  $S(z)$  to monitor the magnetic response of the sample after cooling in a  $H_a$ . Figure 11(a) shows  $S(z)$  measured below  $T_c$  after cooling in the desired  $H_a$  with the sample at  $z=57.5$  mm. We see that the response functions for small  $H_a$  values are highly distorted by the  $H'_r(z)$  between the measuring coils. Referring to Fig. 8, we see that within one of the pickup coils, the response function  $S_{H_a}(z)$  obtained after cooling in the  $H_a$  is  $S_{H_a}(z) = \beta_1(H_a + H_{r2}) + \beta_2[H_r(z) - H_{r2}]$ , which reduces to  $\beta_1 H_a + \beta_2(H_r(z) - H_{r2})$  for  $H_a \gg H_{r2}$ . But the correction function,  $S_{\text{corr}}(z)$ , measured in  $H_a=0$  after cooling at  $z=57.5$  mm, is  $S_{\text{corr}}(z) = \beta_2[H_r(z) - H_{r2}]$ . Thus,  $S_{H_a}(z) - S_{\text{corr}}(z) = \beta_1 H_a$ , the desired response function corrected for  $H'_r(z)$ .

Figure 11(b) shows the measurements of Fig. 11(a) after correcting for the shielding signal resulting from  $H'_r(z)$ ; that is, after subtracting from each curve, the  $S(z)$  response at 57.5 mm obtained after cooling in  $H_a=0$  [Fig. 8(a) at 57.5 mm]. We see that for  $H_a < 8$  Oe, the correction procedure has converted the highly distorted  $S(z)$  measurements [Fig. 11(a)] to the remarkably antisymmetric axial response functions expected from a dipole sample. Of course, the correc-

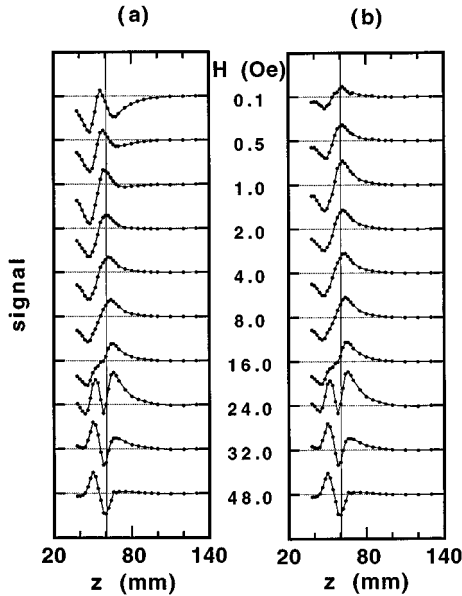


FIG. 11.  $S(z)$  response functions when the sample (KG-y) was cooled, at  $z=57.5$  mm, in the indicated fields. The functions in panel (b) are the functions of panel (a) after correcting for the residual field gradient [curve  $z=57.5$  mm of Fig. 8(a) is subtracted]. For graphical presentation, the curves, from top to bottom, are scaled by the factors: 1, 0.59, 0.58, 0.29, 0.19, 0.13, 0.09, 0.13, 0.06, 0.02.

tions are most profound for small  $H_a$  values, where the FC  $S(z)$  is small and shielding signals from  $H_r$  have a relatively large effect on  $S(z)$ . Figure 11(b) shows that, for  $H_a < 16$  Oe, the symmetry of the  $S(z)$  signals clearly reveals that the samples are paramagnetic.

We note that, for  $H_a < 1$  Oe, the uncorrected FC  $S(z)$  is highly distorted by shielding currents from  $H_r'(z)$  in the measurement volume, even though  $H_r(z)$  is very small (varying by about 4 mOe). The distortion occurs because FC signals are only a few percent, or less, of shielding signals.

For an ideal dipole response, we expect the maximum in  $S(z)$  to appear approximately in the plane of the upper detector coil; i.e., at  $z=60$  mm. However, in Fig. 11(b), we observe that the maximum is not always at  $z=60$  mm. This is an indication of higher multipole components that result

from the flux distribution peculiar to these FC samples.<sup>26</sup> In the vicinity of 24 Oe [Fig. 11(b)], the paramagnetic-diamagnetic crossover region, effects of  $H_a(z)$  introduced by the external field coil might become important. Quadrupole and higher multipole components in the field distribution around the sample that could result from an inhomogeneous flux distribution in the sample, will also contribute to the signal distortion. Thus, while some ambiguity exists in the nature of the magnetic response in the vicinity of the paramagnetic-diamagnetic crossover, it is clear that the signal is paramagnetic at low fields ( $H_a < 10$  Oe) and diamagnetic at high fields ( $H_a > 50$  Oe).

Inhomogeneities in external field coils can also lead to spurious results, especially when the magnetic response of a sample is small in the presence of relatively large  $H_a(z)$ . In Fig. 11, for example, with  $H_a$  near 24 Oe,  $S(z)$  is very weak even though  $H_a$  is quite large. In this case, shielding effects from small  $H_r'(z)$  contributed by the solenoid can become important. That is, shielding signals in  $S(z)$  will again appear as the FC sample is repositioned through  $H_r'(z)$ . Such a gradient could also be responsible for the double-peaked  $S(z)$  appearing at 24 Oe. The peak-to-peak magnitude of the 24 Oe FC  $S(z)$  (Fig. 11) is about twice the peak-to-peak magnitude of the  $H_r$   $S(z)$  [Fig. 8(a)] for  $50 \text{ mm} < z < 60 \text{ mm}$ , which results from a 4 mOe  $H_r'(z)$  between the pickup coils. Thus, a  $H_a'(z)$  of about 10 mOe ( $\sim 0.05\%$  of  $H_a$ ) appearing between the pickup coils apparently could produce the double-peaked structure. The observed sign of  $M(T)$  could be incorrect in the immediate vicinity of the paramagnetic-diamagnetic crossover (near 18 Oe in Fig. 4); i.e.,  $H_a'(z)$  provides some uncertainty in the value of the field where the crossover occurs. While not necessary for this study, it is possible to measure  $H_a'(z)$  using procedures similar to those described above.

Clearly, when measuring with *moving* sample systems, *extreme* care must be taken to ensure that a proper signal response is observed. For SQUID No. 2, this condition was not satisfied for  $H < 5$  Oe. For FC measurements obtained in  $H > 5$  Oe,  $M(H)$  measurements from SQUID No. 2 were comparable to those obtained with SQUID No. 1.  $M(H)$  measured at 10 Oe in SQUID No. 2 was  $4.1 \times 10^{-5}$  emu for sample KG-1, compared to  $4.5 \times 10^{-5}$  emu measured in SQUID No. 1. For both SQUID's, the onset of diamagnetic behavior for the FC measurement appeared with  $H \sim 20$  Oe.

<sup>1</sup>J. R. Clem and Z. Hao, Phys. Rev. B **48**, 13 774 (1993).

<sup>2</sup>P. Svedlindh, K. Niskanen, P. Norling, P. Nordblad, L. Lundgren, B. Lönnberg, and T. Lundström, Physica C **162-164**, 1365 (1989).

<sup>3</sup>W. H. Lee, Y. T. Huang, S. W. Lu, K. Chen, and P. T. Wu, Solid State Commun. **74**, 97 (1990).

<sup>4</sup>W. Braunisch, N. Knauf, V. Kataev, S. Neuhausen, A. Grütz, B. Roden, D. Khomskii, and D. Wohlleben, Phys. Rev. Lett. **68**, 1908 (1992); W. Braunisch, N. Knauf, G. Bauer, A. Kock, A. Becker, B. Freitag, A. Grütz, V. Kataev, S. Neuhausen, B. Roden, D. Khomskii, D. Wohlleben, J. Bock, and E. Preisler, Phys. Rev. B **48**, 4030 (1993).

<sup>5</sup>Ch. Heinzl, Th. Theilig, and P. Ziemann, Phys. Rev. B **48**, 3445 (1993).

<sup>6</sup>S. Riedling, G. Bräuchle, R. Lucht, K. Röhberg, H. v. Löhneysen, H. Claus, A. Erb, and G. Müller-Vogt, Phys. Rev. B **49**, 13 283 (1994).

<sup>7</sup>F. C. Chou, D. C. Johnston, S.-W. Cheong, and P. C. Canfield, Physica C **216**, 66 (1993).

<sup>8</sup>Weiyuan Guan, Appl. Phys. Lett. **66**, 2748 (1995).

<sup>9</sup>F. J. Blunt, A. R. Perry, A. M. Campbell, and R. S. Liu, Physica C **175**, 539 (1991).

<sup>10</sup>M. Sigrist and T. M. Rice, J. Phys. Soc. Jpn. **61**, 4283 (1992); Rev. Mod. Phys. **67**, 503 (1995).

- <sup>11</sup>D. Domínguez, E. A. Jagla, and C. A. Balseiro, *Phys. Rev. Lett.* **72**, 2773 (1994).
- <sup>12</sup>D.-X. Chen and A. Hernando, *Europhys. Lett.* **26**, 365 (1994).
- <sup>13</sup>F. V. Kusmartsev, *Phys. Rev. Lett.* **69**, 2268 (1992).
- <sup>14</sup>D. Khomskii, *J. Low Temp. Phys.* **95**, 205 (1994).
- <sup>15</sup>M. S. M. Minhaj, D. J. Thompson, L. E. Wenger, and J. T. Chen, *Physica C* **235-240**, 2519 (1994); D. J. Thompson, M. S. M. Minhaj, L. E. Wenger, and J. T. Chen, *Phys. Rev. Lett.* **75**, 529 (1995).
- <sup>16</sup>K. G. Vandervoort, G. Griffith, H. Claus, and G. W. Crabtree, *Rev. Sci. Instrum.* **62**, 2271 (1991).
- <sup>17</sup>B. W. Roberts (unpublished).
- <sup>18</sup>R. Lucht, H. v. Löhneysen, H. Claus, M. Kläser, and G. Müller-Vogt, *Phys. Rev. B* **52**, 9724 (1995).
- <sup>19</sup>B. Büchner, P. Schmidt, and D. Khomskii (private communication).
- <sup>20</sup>K. Steiner and H. Schoeneck, *Phys. Z.* **44**, 341 (1943); **44**, 346 (1943).
- <sup>21</sup>W. Meissner, F. Schmeissner, and H. Meissner, *Z. Phys.* **130**, 521 (1951); **130**, 529 (1951).
- <sup>22</sup>M. A. R. LeBlanc, *Phys. Rev.* **143**, 220 (1966).
- <sup>23</sup>F. de la Cruz, H. J. Fink, and J. Luzuriaga, *Phys. Rev. B* **20**, 1947 (1979).
- <sup>24</sup>A. E. Koshelev and A. I. Larkin, *Phys. Rev. B* **52**, 13 559 (1995).
- <sup>25</sup>E. Zeldov, J. R. Clem, M. McElfresh, and M. Darwin, *Phys. Rev. B* **49**, 9802 (1994).
- <sup>26</sup>A. K. Grover, R. Kumar, S. K. Malik, and P. Chaddah, *Solid State Commun.* **77**, 723 (1991).